Preclinical Development

Molecular Cancer Therapeutics

Ovarian Cancer Stem Cell–Like Side Populations Are Enriched Following Chemotherapy and Overexpress *EZH2*

Siân Rizzo[1], Jenny M. Hersey[1], Paul Mellor[1], Wei Dai[4], Alessandra Santos-Silva[1], Daniel Liber[4], Louisa Luk[4,5], Ian Titley[2], Craig P Carden[1], Garry Box[3], David L. Hudson[1], Stanley B. Kaye[1], and Robert Brown[1,4]

Abstract

Platinum-based chemotherapy, with cytoreductive surgery, is the cornerstone of treatment of advanced ovarian cancer; however, acquired drug resistance is a major clinical obstacle. It has been proposed that subpopulations of tumor cells with stem cell–like properties, such as so-called side populations (SP) that overexpress ABC drug transporters, can sustain the growth of drug-resistant tumor cells, leading to tumor recurrence following chemotherapy. The histone methyltransferase EZH2 is a key component of the polycomb-repressive complex 2 required for maintenance of a stem cell state, and overexpression has been implicated in drug resistance and shorter survival of ovarian cancer patients. We observed higher percentage SP in ascites from patients that have relapsed following chemotherapy compared with chemonaive patients, consistent with selection for this subpopulation during platinum-based chemotherapy. Furthermore, *ABCB1* (P-glycoprotein) and *EZH2* are consistently overexpressed in SP compared with non-SP from patients' tumor cells. The siRNA knockdown of *EZH2* leads to loss of SP in ovarian tumor models, reduced anchorage-independent growth, and reduced tumor growth *in vivo*. Together, these data support a key role for *EZH2* in the maintenance of a drug-resistant, tumor-sustaining subpopulation of cells in ovarian cancers undergoing chemotherapy. As such, EZH2 is an important target for anticancer drug development. *Mol Cancer Ther; 10(2); 325–35. ©2010 AACR.*

Introduction

The majority of ovarian cancer patients present with advanced disease. Although up to 80% respond well to surgery and platinum-based chemotherapy, tumor recurrence is a common event (1). Following relapse, treatment with platinum can elicit a further response; however, the duration of response tends to decrease with each round of therapy, as patients develop disease with increased chemoresistance. Subpopulations of tumor cells with stem cell–like properties have been proposed to sustain the growth of tumor cells and the inherent drug resistance of these stem cell–like cells could lead to tumor recurrence following chemotherapy (1, 2). Support for the existence of ovarian tumor stem cells comes from studies examining both tumor biopsies and ascites (3–8). Thus, ovarian tumors contain cells that are capable of prolonged growth in an anchorage-independent manner as spheroids and are tumorigenic when injected at low cell numbers into mice (7). Subpopulations of cells capable of forming tumors in xenogeneic mice have been isolated from ascites of ovarian cancer patients (8).

One widely used method for isolating putative cancer stem cells is based on ABC transporter–mediated efflux of the Hoechst 33342 dye to isolate a side population (SP). This dye-excluding SP phenotype has been shown to be enriched with cancer stem–like cells in a variety of tumors (8–14). Furthermore, SP cells from ovarian cancer ascites can form tumors more readily in mice than non-SP cells following 5 days in culture (8). The presence of SP cells with increased *in vitro* drug resistance has been shown in mouse and human ovarian cancer cell lines (5, 8); although, the relevance to clinical acquired drug resistance is still to be established.

Polycomb group proteins have been shown to be required for the maintenance of embryonic stem cells and could therefore also have a role in maintaining tumor stem/sustaining cells (15–17). Indeed, the key component of polycomb repressive complex (PRC2) EZH2, a specific histone 3 Lys27 (H3K27) methyltransferase, is essential for stem cell maintenance in glioblastoma (18). EZH2 plays a critical role in tumorigenesis and cancer progression through epigenetic gene silencing and chromatin remodeling (19, 20). There is increasing evidence that

Authors' Affiliations: [1]Section of Medicine and Sections of [2]Haemato-oncology and [3]Cancer Therapeutics, Institute of Cancer Research, Sutton, Surrey, United Kingdom; [4]Ovarian Cancer Action Research Centre, Department of Surgery and Cancer, Imperial College London, Hammersmith Hospital Campus, London, United Kingdom; and [5]Bioprocessing Technology Institute Céntros, Singapore

Note: Supplementary material for this article is available at Molecular Cancer Therapeutics Online (http://mct.aacrjournals.org/).

Corresponding Author: Robert Brown, Department of Surgery and Cancer, Hammersmith Campus, Imperial College, London W12 ONN, United Kingdom. Phone: 020-759-41804; Fax: 4420838530. E-mail: r.brown@imperial.ac.uk

doi: 10.1158/1535-7163.MCT-10-0788

overexpression of the *EZH2* gene occurs in a variety of human malignancies including oral, esophageal, gastric, colon, hepatocellular, bladder, breast, prostate, and endometrial cancers (21–23). Putative oncogenic and tumor-suppressive roles for EZH2 have been suggested (24, 25). Elevated expression of EZH2 has been shown to be associated with advanced stages of ovarian cancer and independently associated with short overall survival of ovarian cancer patients (26). Furthermore, EZH2 knockdown in ovarian cell lines leads to reduced cell growth/proliferation and inhibited cell migration and/or invasion *in vitro* (26), as well as resensitization of drug-resistant ovarian cancer cells to cisplatin (27). However, these studies have not examined EZH2 in an ovarian tumor stem cell population derived from patients during clinical acquired resistance.

We have address whether SP cells can be isolated from ascites from ovarian cancer patients and whether the size of the SP subpopulation changes during chemotherapy. Given the observed role of EZH2 in platinum resistance of ovarian cell lines (27), we have examined whether *EZH2* is overexpressed in these tumor-derived SP cells and whether inhibition of *EZH2* may have the potential to inhibit growth of drug-resistant ovarian tumor stem cells.

Materials and Methods

Patient material preparation and cell line culture

Ascitic fluid was obtained from ovarian cancer patients requiring therapeutic paracentesis following informed consent for this study, approved by the Royal Marsden Hospital Ethics Review Committee and the Hammersmith Hospital Ethics Review Committee. Within 24 hours of receipt, ascites were centrifuged at 400 × *g* for 15 minutes to concentrate the cellular content. The concentrated fraction was overlaid onto lymphocyte preparation medium (PAA Laboratories) and centrifuged for 30 minutes at 400 × *g* without braking. Cells at the interface, enriched for tumor cells and lymphocytes, were collected and washed in RPMI 1640 (Invitrogen) + 10% FBS (PAA Laboratories) then centrifuged for 10 minutes at 400 × *g*. Contaminating red blood cells were lysed using a RBC Lysis kit (Miltenyi Biotec Ltd.) according to the manufacturer's instructions.

IGROV1 (28), PEO1, PEO4, PEA1, PEA2, PEO14, PEO23 (29), and OSEC2 (30) were obtained from Ovarian Cancer Action Research Centre, Imperial College, London, UK. All cell lines were maintained in RPMI 1640 + 10% FBS. IOSE21 were obtained from Prof. Frances Balkwill, Institute of Cancer, Centre for Cancer and Inflammation, Barts, and The London School of Medicine and Dentistry, London. Cell lines were shown to be identical to those received on the basis of DNA methylation pattern analyzed within 1 month of use and the methylation patterns showed close similarity between samples from the same patient, otherwise no further authentication was carried out.

Chemotherapeutic treatment of cell lines

Purified cell populations were plated and treated 24 hours later with cisplatin (Sigma-Aldrich), carboplatin (Sigma-Aldrich), and paclitaxel (Sigma-Aldrich) for 24 hours. The medium was replaced and the cells were allowed to recover for 48 hours then survival was assessed by MTT assay or the change in SP was measured by flow cytometry following cell enumeration by hemocytometer.

Flow cytometry

Hoechst 33342 staining of cells (22) in combination with immunophenotyping. Cells were resuspended at 10^6/mL RPMI 1640 + 2% FBS, 10 mmol/L HEPES (Sigma-Aldrich), and 5 μg/mL Hoechst 33342 then incubated at 37°C with rotation, optimal incubation times were determined for each cell line. Cells were washed in 4 volumes of analysis buffer consisting of ice-cold HBSS containing 2% FBS and 10 mmol/L HEPES. Cells were analyzed and sorted using a BD FACS VantageSE DiVa equipped with 2 Coherent Innova 90 lasers, one with visible optics tuned to 488 nm and set to 200 mW and one with UV optics emitting multiline UV 333.6 to 363.8 nm set to 50 mW. Sheath fluid was sterile PBS (pH 7.2; in-house) and cells were sorted with sheath pressure set at 12 psi (0.82 bar). On reanalysis of sorted populations, the purity generally exceeded 90%. To confirm the presence of an SP and define the gate for cell sorting, verapamil was added to control samples at a final concentration of 20 μmol/L.

For primary ascites cells, CD45-FITC (Fluoroscein isothiocyanate; Clone HI30; BD Biosciences) and/or CD326-APC (EpCAM, Clone HEA-125, Miltenyi Biotech) was added to the cells for 30 minutes on ice and the excess removed by washing, appropriate matched isotype controls were also used to identify nonspecific labeling. Cells were resuspended in HBSS (Invitrogen) containing 2% FBS and 2 μg/mL propidium iodide (Sigma-Aldrich) then analyzed and sorted as described above. Data were analyzed using FCS Express Professional version 3 (De Novo Software).

In vivo grafts

All procedures were approved by the Institute of Cancer Research Ethics committee and all work performed in accordance with UK Home Office regulations under the Animals (Scientific Procedures) Act 1986 and UKCCR guidelines for animal experimentation (30). SP and non-SP from IGROV1 cells were sorted as described above and resuspended in ice-cold 50% Matrigel (BD biosciences) in RPMI 1640 at 50 μL per xenograft. Between 50 and 250 cells were injected into the mammary fat pad of 10-week-old NOD/SCID mice (Charles River) and allowed to grow for up to 12 weeks. Unsorted cells were grafted as a positive control for cell viability and graft take. Similarly, 48 hours post-siRNA treatment, IGROV1 cells were harvested using TrypLE and counted, 50 μL grafts were prepared and transplanted as described

above, using 250 cells per graft. Tumor size was monitored by calliper measurements across 2 diameters (d) at regular intervals to calculate tumor volume (cm^3) = $4/3\pi [(d_1 + d_2)/4]^3$.

Spheroid forming assays

Cells were plated at a range of densities in 6-well ultralow adhesion tissue culture plates in 2 mL RPMI 1640) + 10% FBS and transferred to an incubator with supplementary feeding with same media and serum every 3 to 4 days. Spheroids were allowed to form for 18 days and then counted. In some cases, spheroids were transferred to adherent plates. The adhered spheroids were fixed in 3.7% formalin in PBS then stained with 1% rhodamine B in water. Images of each well were captured then analyzed by Image-Pro Analyser 6.3 to quantitate colony size and frequency.

siRNA treatment

Optimal plating densities were determined to allow proliferation for up to 96 hours for each cell line. Protocols were optimized as recommended by the manufacturer's instructions. siRNAs were delivered using HiPerfect (Qiagen) within 16 hours of plating cells. All experiments consisted of untreated controls, mock controls, control siRNA (Allstars scrambled siRNA, Qiagen), and positive control siRNA (MAPK, Qiagen).

RNA preparation, reverse transcription, and quantitative real-time PCR

Total cellular ribonucleic acid (TRNA) was extracted (RNeasy Minikit Plus, Qiagen) and quantified by measurement of optical density at $OD_{\lambda 260}$. Up to 2 μg of RNA was reverse transcribed and first-strand cDNA synthesized in 40 μL using the Superscript II reverse transcriptase kit (Invitrogen) according to manufacturer's instructions. Samples were amplified using TaqMan gene expression assays (Applied Biosystems) and a Step One PCR machine (Applied Biosystems). TaqMan probe and primers (see manufacturer's website) were used: ABCB1 (assay ID Hs01067802_m1), ABCG2 (assay ID Hs01053790_m1), GAPDH (part no 4326317E), EZH1 (assay ID Hs00157470_ml), and EZH2 (assay ID Hs01016789_ml).

Histone extraction and immunoblotting

Cells were resuspended in lysis buffer [PBS containing 0.5% Triton X-100 (v/v), 1× complete protease inhibitor cocktail; Roche] and left to lyse for 10 minutes at 4°C. Nuclei were then precipitated and resuspended in 0.2N HCl overnight at 4°C. Nuclear debris were pelleted and the supernatant recovered. Protein concentration was calculated by Bradford assay (Bio-Rad). The lysate was separated by 8% to 16% SDS-PAGE and transferred to nitrocellulose membranes. Rabbit polyclonal antibodies anti-trimethyl-histone-H3 (Lys27, 07-449; Millipore) was used for immunoblotting.

Microarray hybridization and Gene Set Analysis

Gene expression in 3 independently sorted SP and non-SP from IGROV1 cells exponentially growing under standard tissue culture conditions was determined by Affymetrix array using the HG-U133plus2 GeneChip array following amplification labeling. Labeling and hybridizations were carried out at the Paterson Institute Microarray Facility (Manchester, UK) following standard protocols. Full methods are available at http://bioinformatics.picr.man.ac.uk/mbcf.

The raw expression data of IGROV1 SP and non-SP in Affymetrix HG-U133plus2 microarrays were normalized as previously described (31) excluding the probes with low signal intensities (average expression across all the samples <25th quantile of the whole data set). The data have been deposited in NCBI's Gene Expression Omnibus and are accessible through GEO Series accession number GSE25191 (http://www.ncbi.nlm.nih.gov/geo/query/acc.cgi?acc=GSE25191). Expression values of multiple probes targeting the same gene were averaged, resulting in a total of 20,323 unique genes in Gene Set Analysis (GSA; ref. 32) to assess the differential expression between 3 pairs of SP and non-SP cells in 15 predefined characteristic signatures that embryonic stem cells have. We computed the gene scores (t-statistic z_i) for all the genes in one gene set S. The larger absolute value of the average of the positive and of the negative parts of each z_i in S is called "maxmean statistic". The significance of the "maxmean statistic" in each gene set was determined by false discovery rate (FDR), estimated on the basis of row randomization and label permutation. FDR less than 5% was used to determine the enrichment of upregulation/downregulation of those signatures in SP cells. This analysis was done in R (version 2.8.1) using GSA package (33).

Statistical analysis

All further analyses were performed using the statistical analysis package GraphPad Prism v5 (GraphPad Software Inc.). The significant level was set at 2-sided $P < 0.05$. All figures are shown with means and standard errors unless otherwise stated.

Results

SP cells from IGROV1 ovarian tumor cell line have tumor stem cell–like properties

ABC transporter–mediated efflux of the Hoechst 33342 dye to isolate a dye-excludings SP has been shown to be enriched for cells with cancer stem–like properties in a variety of tumors (8-14). SP cells from ascites of ovarian cancer patients have been shown to form tumors more readily in mice than non-SP cells (8). Using differential Hoechst 33342 staining of cells to identify SP of the IGROV1 ovarian tumor cell line, we observe significantly increased tumorigenicity (Repeated measures ANOVA: $P < 0.05$) of SP compared with non-SP cells when injecting 50 or 100 cells into the mammary fat pad of NOD/SCID

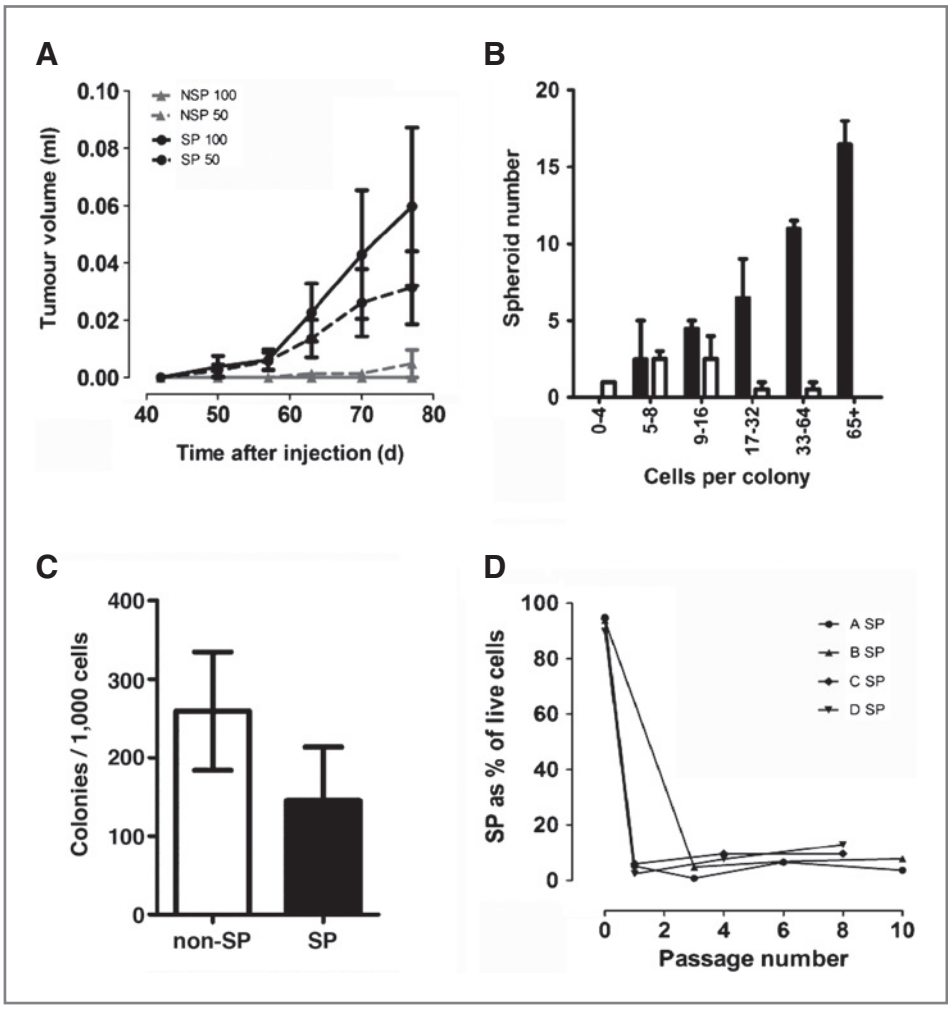

Figure 1. Tumor formation and anchorage-independent growth of SP cells. A, when injected at low cell doses (50 or 100 cells, $n = 6$–8 per group) in Matrigel into the NOD/SCID mammary fat pad, IGROV1 SP cells formed tumors more frequently than non-SP (NSP) cell and produced significantly larger tumors over the duration of the experiment (repeated measures ANOVA: $P < 0.05$, error bars, standard errors). B, following FACS selection, SP (solid bars) and non-SP cells (open bars) were allowed to form spheroids in nonadherent culture for 18 days and were transferred to adherent plates to determine colony size. SP cells produced spheroids with a greater frequency and larger size than non-SP cells C, SP and non-SP were selected by FACS and plated at low density in adherent culture, colonies were counted after 10 days. Colony formation by non-SP was significantly greater than by SP ($P = 0.0092$, paired Student's t test). D, IGROV1 SP and non-SP were sorted (biological replicates: $n = 4$, mean purity 93.3%) and subsequently maintained in adherent culture through 8 to 10 passages. The cells were harvested at intervals and the size of the SP was measured by FACS. The SP fell rapidly and stabilized to levels similar to the original unsorted levels in all cases.

mice (Fig. 1A). In addition to the differences in average tumor growth, SP cells initiated tumors more frequently (8/14 injections) than non-SP (1/12) injections (Fisher's exact test: $P = 0.0145$). Furthermore, SP cells have a greater ability to grow in an anchorage-independent manner as spheroids compared with non-SP (Fig. 1B). The differences in growth properties of SP and non-SP cells could be due to toxicity of Hoechst 33342 and its increase accumulation in non-SP cells. Arguing against this interpretation, we observe non-SP IGROV1 cells to have in fact significantly increased plating efficiency compared with SP cells in standard adherent two-dimensional tissue culture assays (Fig. 1C) and the enhanced growth of SP was only observed in anchorage-independent spheroid growth conditions (Fig. 1B). Asymmetric division is a key feature of stem cells (34). To examine whether isolated SP cells could repopulate SP and non-SP cell populations, multiple SP IGROV1 populations were isolated by FACS (fluorescence-activated cell sorter) and continuously cultured for up to 10 passages. The number of SP cells in the SP selected cultures declined rapidly on passaging with an increase in non-SP cells (Fig. 1D). The mean purity of SP cells following initial separation was 93.3%. It could be argues that a higher proliferative capacity of the contaminating non-SP could lead to the rapid re-emergence of the non-SP. However, the SP became stable as a minority of the total population and the cell culture retained SP and non-SP equivalents to the proportions present in the original cell line. Furthermore, whereas the growth potential of the SP is slightly reduced compared with the non-SP (Fig. 1C), this is unlikely to explain the rapid emergence of the non-SP cells.

GSA (32) was used to interrogate gene expression profiling of SP compared with non-SP from IGROV1 cells for 15 published embryonic stem cell related signatures (Supplementary Table 1). Four signatures with $P < 10^{-6}$ and FDR greater than 10^{-4} were significantly upregulated in SP compared with non-SP: Oct4-regulated genes, NOS signature (Nanog/Oct4/Sox2-regulated genes), E2F6-associated expression pattern, and PRC2. Consistent with upregulation of *PRC2* genes, the PRC2 target genes were significantly repressed in the SP ($P < 10^{-6}$ and FDR $< 10^{-4}$). The individual GSA scores for the PRC2 target genes are shown in Supplementary Table 4. Thus,

on the basis of cell phenotype and overrepresentation of stem cell gene expression patterns, SP cells isolated from the IGROV1 human ovarian tumor cell line have tumor stem cell–like properties.

The proportion of SP in ovarian cancer ascites increases following chemotherapy

We assessed the relative proportion of SP cells present in tumors from ovarian cancer patients. We measured the proportion of SP cells present in EpCAM-positive, CD45-negative tumor cells in patient ascites collected either at initial presentation or at relapse after platinum-based chemotherapy (Table 1). Ascites samples collected from relapsed patients show a significant ($P = 0.013$) increase in proportion of SP cells compared with chemonaive patients (Fig. 2A). Patients were categorized, postascitic drainage, as having either disease control (partial response or stable disease) or progressive disease to subsequent chemotherapy (Table 1). Those with progressive disease tended to have increased SP (mean = 1.8 ± 0.9) compared with those with disease control (mean = 0.42 ± 0.24, $P = 0.055$, unpaired Student's t test with Welch's correction).

Sequential ascites samples taken from 3 patients during treatment show progressive increase in the SP (Table 1). We have also examined the proportion of SP present in matched cell lines derived from patients' tumors at diagnosis and at platinum-resistant relapse (Table 2). These lines have previously been shown to acquire *in vivo* increased resistance to carboplatin during chemotherapy (29) and represent isogenic models of clinical drug resistance. We observe an increase in the percent SP in all three of the lines that have acquired platinum resistance compared with the matched chemosensitive tumor line. Two immortalized cell lines generated from normal surface ovarian epithelial cells did not contain a detectable SP.

Carboplatin selects for increased SP *in vitro*

The increase in SP observed with development of chemoresistance following carboplatin-based chemotherapy argues that SP cells may have a selective survival or growth advantage during chemotherapy. Resistance of tumor stem cells to chemotherapeutic drugs has previously been described in a variety of tumor types including ovarian cancer SP (8, 35). Indeed, we observe increased resistance of IGROV1 SP compared with non-SP to platinum (cisplatin and carboplatin) and to paclitaxel (Fig. 3A). However, it could be argued that this differential drug sensitivity is influenced by differential levels of Hoechst dye remaining in the SP and non-SP cells. Therefore, we examined whether exposure of IGROV1 cells to physiologically relevant levels of carboplatin (in the absence of Hoechst dye) could select for an increased proportion of SP cells. As shown in Figure 3B, SP cells remain relatively unaffected by the carboplatin treatment, whereas there is a significant decrease in viability of the non-SP, consistent with the effects of carboplatin on the viability of the bulk population of cells. The net effect will be an enrichment or selection for the SP cell population during platinum exposure.

Differential expression of ABC transporters has been widely observed in SP from a variety of tumor types; although, in the majority of studies, overexpression of ABCG2 is observed (8, 35). Real-time (RT) PCR quantification of *ABCB1* and *ABCG2* mRNA showed that *ABCB1* was overexpressed in SP cells in comparison with non-SP cells from 4 of 5 ovarian cancer cell lines and in primary patient ascites ($n = 10$), whereas *ABCG2* was below the level of quantification by RT-PCR, except for PEA2, from which *ABCB1* was absent (Table 3). Carboplatin is not a substrate for P-glycoprotein (36) and therefore overexpression of *ABCB1* is unlikely to be the explanation of the increased resistance to carboplatin or selection of SP cells observed. Because ABCC5 and ABCC6 have been implicated in cisplatin resistance (37, 38), we specifically examined by qRT-PCR (quantitative RT-PCR) their levels in SP and non-SP from patient ascites; but, in the case of *ABCC5*, no significant difference was observed (1.22 SP to non-SP ratio, $n = 10$) and for *ABCC6*, the levels were undetectable in SP and non-SP ($n = 10$). Paclitaxel is a substrate for ABCB1 and therefore overexpression of *ABCB1* in this subpopulation could affect the likelihood of relapse following taxane containing chemotherapy; however, we do not observe increased resistance of the SP cells compared with non-SP for paclitaxel sensitivity (Fig. 3A).

Increased expression of EZH2 in SP from patient ascites compared with non-SP

PRC2 contains the histone methyltransferase EZH2, which, together with EED and SUZ12, trimethylates histone H3 on Lys27 (H3K27me3) and is associated with a repressive chromatin state (20). EZH2 is overexpressed in many cancers and levels of EZH2 correlate with poor prognosis including ovarian cancer (21–23, 26). We observe increased expression of EZH2 in 7 of 10 SP compared with non-SP isolated from ascites in patients with recurrent ovarian cancer (Table 4), with up to 14-fold increase expression in SP compared with non-SP in patient samples. The increased EZH2 expression observed in SP from patient ascites is variable and may represent differences in purity of the FACS-sorted SP, although there is no obvious correlation with level of ABCB1 (Table 4). Previous studies have suggested that differential levels of Hoechst dye can affect gene expression in SP cells (39). We observed no effect of Hoechst dye on EZH2 levels or ABCB1 levels (data not shown).

Knockdown of EZH2 and EZH1 in ovarian tumor cell lines reduces SP and tumor stem cell–like phenotype.

Propagation of the H3K27me3 mark during cell division accounts for the maintenance and somatic inheritance of repressive chromatin domains (40). Therefore, inhibition of EZH2 should reduce H3K27 methylation levels, leading to gene reactivation. To examine whether

Table 1. Ascites collected from ovarian cancer patients: SP and clinical details at time of ascites collection and response to subsequent chemotherapy

Sample number	Age, y	Stage	Grade	Histology	Most recent chemotherapy	% SP ($EpCAM^+/CD45^-$)	At time of ascites collection		Treatment subsequent to ascites collection		
							Lines of chemo-therapy	Response to most recent chemotherapy	Chemotherapy	Response to subsequent chemotherapy	Duration of response, mo
1	68	4	3	Serous adenocarcinoma	Nil	≤0.0001	0	N/A	Carboplatin	PR	3.5
2	64	3c	2	Serous adenocarcinoma	Nil	≤0.0001	0	N/A	Carboplatin/ paclitaxel	PR	5.0
3	62	3c	3	Serous adenocarcinoma	Nil	0.1746	0	N/A	Carboplatin/ paclitaxel	PR	5.0
4	57	4	3	Serous adenocarcinoma	Nil	0.1000	0	N/A	Nil	-	-
5	66	3	NK	NK	Nil	0.0007	0	N/A	Carboplatin/ paclitaxel	PR	2 ongoing
6	74	3	NK	NK	Paclitaxel	2.7392	1	PD	Carboplatin/ paclitaxel	PD	PD
7	75	3	3	Serous adenocarcinoma	Carboplatin	-	1	PD	Paclitaxel	PD	PD
8	59	3c	2	Serous adenocarcinoma	Carboplatin/paclitaxel	0.1874	2	SD	Liposomal doxorubicin	PD	PD
9	62	3	3	Serous adenocarcinoma	Carboplatin/paclitaxel	0.0650	2	SD	Carboplatin/ paclitaxel	PD	PD
10	58	3c	2	Adenocarcinoma	Liposomal doxorubicin	6.7880	3	PD	Nil	-	-
11[a]	62	3c	1	Papillary serous adenocarcinoma	Carboplatin/paclitaxel	0.0093	3	SD	Nil	-	-
12[a]	62	3c	1	Papillary serous adenocarcinoma	Carboplatin/paclitaxel	0.1902	3	SD	Nil	-	-
13	61	4	3	Serous adenocarcinoma	Paclitaxel	0.0036	3	PD	Etoposide	PD	PD
14	77	3	NK	Serous adenocarcinoma	Carboplatin	2.5647	3	PR	Phase I trial	PD	PD
15[a]	54	3	2	Mullerian serous adenocarcinoma	Paclitaxel	0.0044	4	PD	Nil	-	-
16[a]	56	3/4	3	Serous adenocarcinoma	Cisplatin	1.7200	5	SD	Phase I trial	PD	PD
17	75	3	NK	Adenocarcinoma	Paclitaxel	0.0242	6	PD	Carboplatin	PD	PD
18[a]	56	3/4	3	Serous adenocarcinoma	Liposomal doxorubicin	3.3400	7	PD	Nil	-	-
19[a]	54	3	2	Mullerian serous adenocarcinoma	Paclitaxel	0.6536	7	PD	Nil	-	-
20	73	3c	NK	Adenocarcinoma	Carboplatin	0.0586	9	SD	Megesterol	SD	5 (ongoing)

NOTE: Partial response was assessed radiologically using RECIST 1.1 criteria by repeat imaging (generally CT scan).

Abbreviations: NK, not known, information not available from patient notes of histology records; SD, stable disease; PD, progressive disease; PR, partial response.

[a]Indicates paired ascites samples from 3 patients collected 1 week to 2 months apart during chemotherapy.

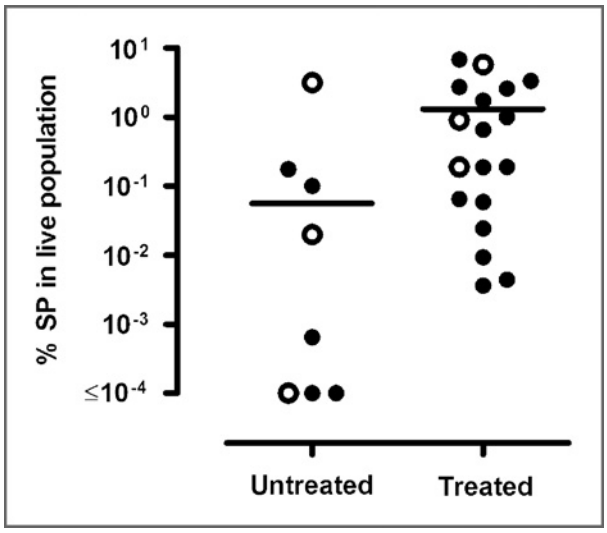

Figure 2. Percent SP in ovarian tumor samples. Percent SP was significantly ($P = 0.0126$, unpaired Student's t test with Welch's correction) lower in freshly isolated patient ascites (solid symbols) from untreated patients ($n = 5$) compared with postchemotherapy ascites ($n = 15$). Open circles are mean percent SP in isogenic-matched prechemotherapy and postchemotherapy cell lines.

Table 2. Percent SP in 3 pairs of isogenic cell lines derived from patients tumors with chemoresponsive or chemoresistant disease

Ovarian tumor cell line	Source of cell line	Mean %SP
PEO1	Patient chemoresponsive to cisplatin, 5FU and chlorambucil	<0.01 (n=5)
PEO4	Same patient as PEO1 after development of clinical resistance	0.90 (n=6)
PEA1	Untreated chemoresponsive patient	0.02 (n=7)
PEA2	Same patient as PEA1 on relapse after carboplatin and prednimustine	0.19 (n=6)
PEO14	Untreated chemoresponsive patient	3.14 (n=7)
PEO23	Same patient as PEO23 on relapse after carboplatin and chlorambucil	5.75 (n=3)
IGROV1	Ovarian tumor	0.75 (n=10)
IOSE21	Normal ovarian surface epithelium	<0.01 (n=4)
OSEC2	Normal ovarian surface epithelium	<0.01 (n=4)

NOTE: Immortalized normal ovarian surface epithelium had undetectable SP.

EZH2 has a direct role in maintaining an SP, we performed siRNA knockdown of *EZH2* in 3 independent ovarian tumor cell lines. *EZH2* knockdown consistently reduced *EZH2* mRNA by greater than 70% and produces a dramatic and prolonged reduction in the levels of H3K27 trimethylation in cells (Fig. 4A).

Because EZH1 also mediates methylation on histone H3 Lys27 and complements EZH2 in maintaining stem cell identity and executing pluripotency (41), we performed double knockdowns of *EZH2* and *EZH1*, as well as *EZH2* alone, in case of potential redundancy of functional effects on tumor stem cells. *EZH2* knockdown alone, or when combined with *EZH1* knockdown, consistently reduced the SP in independent ovarian tumor cell lines (Fig. 4B and C). SP compared with non-SP cells have a greater ability to grow in anchorage-independent culture and form large (>32 cell) spheroids (Fig. 1B). Loss of anchorage-independent growth following knockdown of *EZH2* alone or combined with *EZH2* in IGROV1, PEO14, and PEO23 is observed (data for IGROV1 shown in Fig. 4D). As well as for the pool of 4 siRNAs for *EZH2*

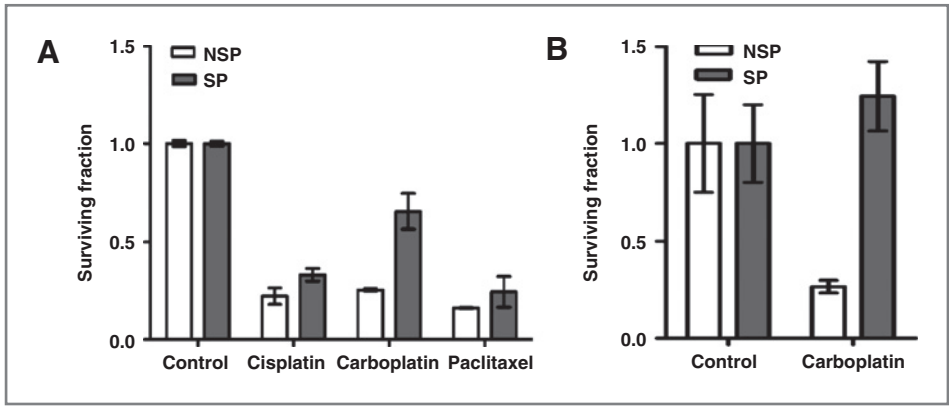

Figure 3. Chemosensitivity of SP. A, chemosensitivity of isolated SP and non-SP (NSP) from IGROV1 at IC_{80} of unseparated cells to cisplatin, carboplatin, and paclitaxel, expressed as a surviving fraction of the control (SP vs. non-SP, cisplatin $P = 0.059$, carboplatin $P = 0.01$, paclitaxel $P = 0.12$, respectively, one-way paired Student's t test). B, unselected IGROV1 cells were treated with carboplatin at 60 μmol/L. Following 48 hours of recovery, SP and non-SP were measured by FACS to calculate the surviving fractions relative to untreated controls. The surviving fraction of SP was significantly greater than the non-SP–surviving fraction ($P = 0.011$, one-way paired Student's t test).

Table 3. Gene Expression of ABCB1 and ABCG2

	IGROV1 (*n*=6)	PEO23 (*n*=3)	PEO14 (*n*=3)	PEA2 (*n*=3)	PEO4 (*n*=3)	Ascites (*n*=10)
ABCB1	14.35	3.75	3.16	Below Quantification	1.85	20.4
ABCG2	Below Quantification	Below Quantification	Below Quantification	5.74 (*n*=2)	Below Quantification	Below Quantification

NOTE: SP and non-SP cells were selected to greater than 90% purity by FACS. Gene expression of ABCB1 and ABCG2 was quantified by RT-PCR from 5 ovarian cancer cell lines and 10 patient ascites. All samples showed enrichment of ABCB1 mRNA expression SP compared with non-SP, with the exception of PEA2 where ABCG2 was overexpressed in the SP (below quantification, mRNA below minimum level for reliable quantification by RT-PCR. All values were normalized to GAPDH, glyceraldehyde 3 phosphate dehydrogenase).

shown in Figure 4D, similar reduction in SP and spheroid growth was observed for all 4 siRNAs when tested individually. Following siRNA knockdown of *EZH1* + *EZH2*, IGROV1 or PEO23 cells were injected into a NOD/SCID mouse model and tumor growth measured. Although knockdown will be transitory and not maintained throughout the xenograft experiment, reduced expression of *EZH2* and reduced H3K27me is observed 48 to 96 hours following SiRNA treatment, the important time frame for tumor take. Despite the transitory nature of the SiRNA knockdown, a persistent reduction in tumor volume in the *EZH2* + *EZH1* knockdowns compared with the controls was observed (Fig. 4E and F).

Discussion

In support of the existence of tumor stem cell–like cells in ovarian tumors, subpopulations of tumor-initiating or -sustaining cells have been identified which grow more readily in an anchorage-independent manner and as tumors in xenogeneic mice (3–8). These subpopulations can be shown to overexpress stem cell–associated markers and to be more resistant to drugs used in the treatment of ovarian cancer (7, 8). One of the methods that has been successfully used to isolate such putative tumor stem cells is differential Hoechst dye uptake (8–13). Using this approach, we have identified a subpopulation of cells from ovarian cell lines that have a more aggressive phenotype, as defined by anchorage-independent growth and tumor formation in NOD/SCID mice, and are resistant to carboplatin and paclitaxel. Consistent with the *in vitro* observation of a survival advantage of SP following exposure to carboplatin and hence potential drug selection, we observe increased SP in tumor cells isolated from patient ascites following chemotherapy and at relapse compared with chemonaive patients.

Table 4. EZH2 mRNA levels in SP and non-SP from ovarian tumor ascites samples

Patient ascites sample number	Ratio of expression of ABCB1 mRNA SP:non-SP	Ratio of expression of EZH2 mRNA SP:non-SP
6	12.9	14.5[a]
7	3.1	4.2[a]
9	10.3	1.3
10	2.9	1.3
14	57.6	3.4[a]
16	8.4	5.9[a]
17	16.9	8.6[a]
18	3.7	1.6[a]
19	36.8	1.1
21	51.8	2.1[a]

[a]Significant ($P < 0.05$) difference in EZH2 expression in SP compared with non-SP.

SP isolated from ovarian tumor cell lines overexpress a NOS cell signature, frequently associated with embryonic stem cells (17). Furthermore, we show that SP isolated from IGROV1 SP overexpress *PRC2* genes, while consistent with this PRC2 repressed targets are underexpressed. PRC2 contains the histone methyltransferase EZH2, which, together with EED and SUZ12, trimethylates histone H3 on Lys27 (H3K27me3) and is associated with a repressive chromatin state (20). Many genes in cancer, including tumor suppressor genes, are epigenetically silenced by mechanisms associated with H3K27me3 which can be independent of DNA methylation (42). Because H3K27me3 is somatically inherited during cell division (40), this argues that it truly is an epigenetic mark that is maintained and as such is a key target for reversing aberrant epigenetic silencing. Consistent with the data presented in our current study in ovarian cancer, EZH2 has been shown to be essential for glioblastoma cancer stem cell maintenance (18). EZH2 is overexpressed in many cancers and levels of EZH2 correlate with poor prognosis in various cancers including ovarian cancer (21–23, 26).

Our data suggest that EZH2 has a key role in maintenance of the drug-resistant SP subpopulation in ovarian

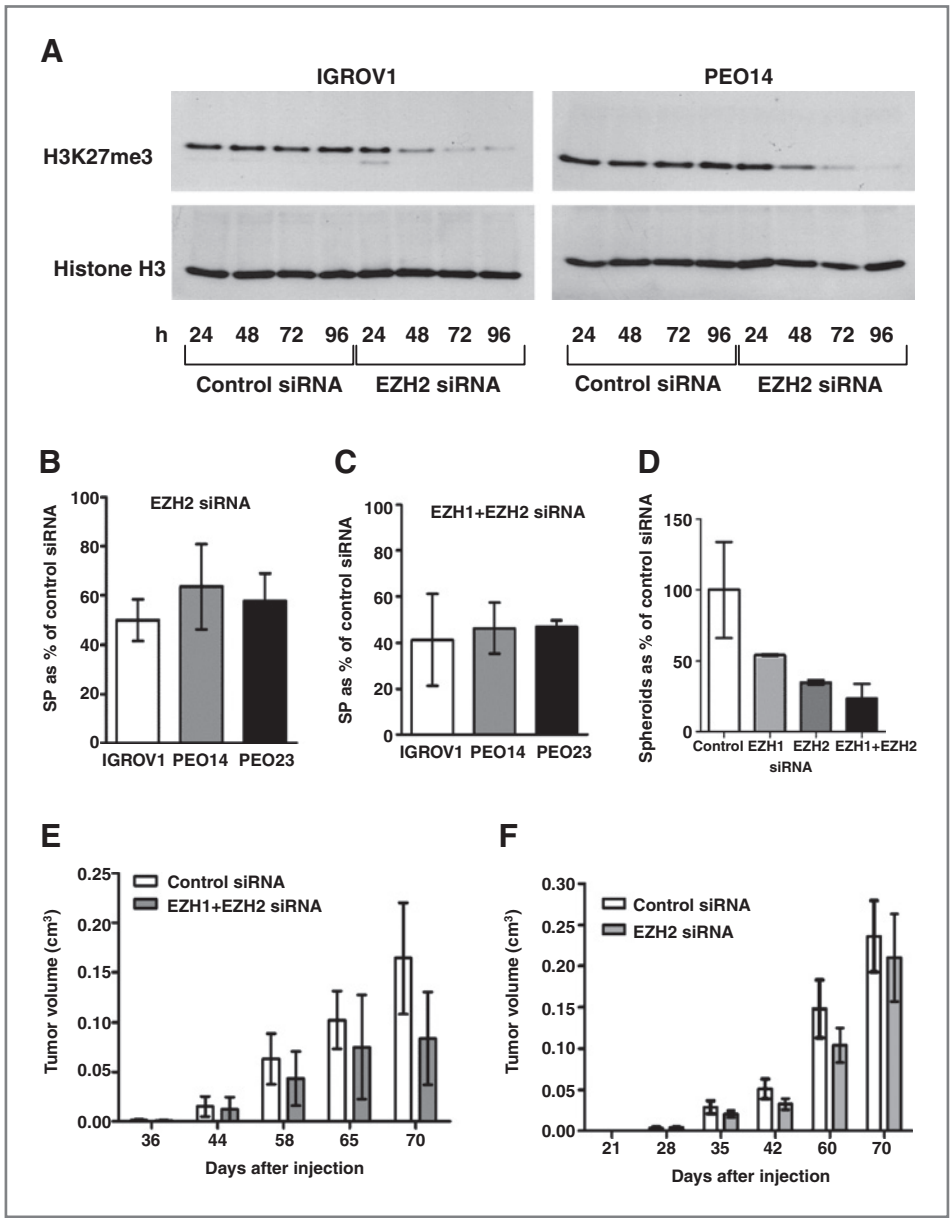

Figure 4. EZH2 knockdown in ovarian cell lines. For all experiments, we confirmed the activity of siRNA used by their ability to knockdown expression of EZH1 and EZH2 using qRT-PCR, achieving 78% to 85% reduction in EZH2 mRNA by 48 to 72 hours for IGROV1 and 72% to 79% for the other lines, while EZH1 mRNA was reduced by 61% to 72% in IGROV1 and 57% to 62% for the other lines. Inhibition of EZH2 mRNA also resulted in reduced protein expression as confirmed by Western blot analysis and by immunofluoresence that also demonstrated nuclear localization of EZH2 protein. Finally, reduced histone methyltransferase activity was demonstrated by time-dependent reduction of H3K27 methylation levels, as shown by immunoblotting analysis (A, top). No effect on the total levels of histone H3 were detected (A, bottom). SP was measured by FACS following EZH2 alone siRNA knockdowns (B) or EZH1 and EZH2 siRNA knockdowns (C) expressed as a percentage of scrambled siRNA controls (mean $\pm$ SEM, $n = 3$ for each cell line). (Pooled data for all cell lines: paired Student's t test $P = 0.0044$, $P = 0.028$, respectively). D, IGROV1 cells were treated with siRNA and allowed to form spheroids for 18 days and then counted ($n = 3$). EZH1- and EZH2-reduced spheroids formation, alone and in combination, EZH2 inhibiting formation to a greater extent than EZH1 alone. IGROV1 cells (E) or PEO23 cells (F) were treated with scrambled control siRNA or EZH1 + EZH2 siRNA *in vitro,* then grafted into the mammary fat pad of NOD/SCID mice at 250 cells per graft. ($n = 6$ per group). Mean tumor volume was determined at regular intervals for up to 10 weeks: mean graft volume was persistently smaller following EZH1 + EZH2 over the duration of the experiment (for IGROV1, $P = 0.072$ and for PEO23, $P = 0.032$, one-way Student's t test).

tumor cells. We have shown that EZH2 is overexpressed in SP derived from ovarian cancer ascites at relapse. EZH2 knockdown in ovarian cell lines has been shown to lead to reduced cell growth/proliferation, as well as cell migration and/or invasion *in vitro* (26), whereas overexpression of EZH2 has been associated with acquired cisplatin resistance (27). Furthermore, loss of H3K27 trimethylation has been shown to result in resensitization of ovarian cancer cells to cisplatin (43); although, lower H3K27 trimethylation levels were

associated with shorter overall survival. (44). However, these previous studies have not examined EZH2 in an ovarian tumor stem cell population derived from patients during clinical acquired resistance, and our present data strongly support the clinical relevance of EZH2 in this important subpopulation of cells selected for during chemotherapy. This drug-resistant subpopulation will be important to eradicate if we aim to improve the treatment of ovarian cancer. Catalytic site inhibitors of histone methyltransferase (45), have been reported, as has indirect pharmacologic inhibition of PRC2 (46), but so far no specific EZH2 inhibitor has been described. Development of specific inhibitors of EZH2 will have potential as drugs that target this key subpopulation of drug-resistant tumor-sustaining cells.

Disclosure of Potential Conflicts of Interest

No potential conflicts of interest were disclosed.

Acknowledgments

With thanks to all those involved in tissue and patient data collection, including Debbie Tandy, Nicole Martin, Nona Rama, Amy Ford, Michelle Everard, Claudia Hayford, Tim Crook, and Matthew Ng as well as the entire gynacological clinical trials team at Hammersmith Hospital headed by Professor Hani Gabra.

Grant Support

This work was supported by Ovarian Cancer Action (S. Rizzo, P. Mellor, R. Brown) and Cancer Research UK (W. Dai, J. Hersey A. Santos-Silva, R. Brown) grants (C536/A6689), Cancer Research UK Experimental Cancer Medicine Centre, The Biomedical Research Council of the Agency for Science, Technology and Research, Singapore (L. Luk), and Leukaemia Research Fund (I. Titley) and Institute of Cancer Research (I. Titley, D.L. Hudson, R. Brown, S.B. Kaye).

The costs of publication of this article were defrayed in part by the payment of page charges. This article must therefore be hereby marked *advertisement* in accordance with 18 U.S.C. Section 1734 solely to indicate this fact.

Received August 24, 2010; revised November 17, 2010; accepted December 2, 2010; published OnlineFirst January 7, 2011.

References

1. Agarwal R, Kaye SB. Ovarian cancer: strategies for overcoming resistance to chemotherapy. Nat Rev Cancer 2003;3:502–6.
2. Dean M. ABC transporters, drug resistance, and cancer stem cells. J Mammary Gland Biol Neoplasia 2009;14:3–9.
3. Ferrandina G, Bonanno G, Pierelli L, Perillo A, Procoli A, Mariotti A, et al. Expression of CD133-1 and CD133-2 in ovarian cancer. Int J Gynecol Cancer 2008;18:506–14.
4. Bapat SA, Mali AM, Koppikar CB, Kurrey NK. Stem and progenitor-like cells contribute to the aggressive behavior of human epithelial ovarian cancer. Cancer Res 2005;65:3025–29.
5. Szotek P P, Pieretti-Vanmarcke R, Masiakos PT, Dinulescu DM, Connolly D, Foster R, et al. Ovarian cancer side population defines cells with stem cell-like characteristics and Mullerian Inhibiting Substance responsiveness. Proc Natl Acad Sci U S A 2006;103:11154–59.
6. Moserle L, Indraccolo S, Ghisi M, Frasson C, Fortunato E, Canevari S, et al. The side population of ovarian cancer cells is a primary target of IFN-alpha antitumor effects. Cancer Res 2008;68:5658–68.
7. Zhang S, Balch C, Chan MW, Lai H, Matei D, Schilder JM, et al. Identification and characterization of ovarian cancer-initiating cells from primary human tumors. Cancer Res 2008;68:4311–20.
8. Hu L, McArthur C, Jaffe RB. Ovarian cancer stem-like side-population cells are tumourigenic and chemoresistant. Br J Cancer 2010; 102:1276–83.
9. Wang J, Guo LP, Chen LZ, Zeng YX, Lu SH. Identification of cancer stem cell-like side population cells in human nasopharyngeal carcinoma cell line. Cancer Res 2007;67:3716–24.
10. Kondo T, Setoguchi T, Taga T. Persistence of a small subpopulation of cancer stem-like cells in the C6 glioma cell line. Proc Natl Acad Sci U S A 2004;101:781–6.
11. Hirschmann-Jax C, Foster AE, Wulf GG, Goodell MA, Brenner MKA. distinct "side population" of cells in human tumor cells: implications for tumor biology and therapy. Cell Cycle 2005;4:203–5.
12. Haraguchi N, Utsunomiya T, Inoue H, Tanaka F, Mimori K, Barnard GF, Mori M. Characterization of a side population of cancer cells from human gastrointestinal system. Stem Cells 2006;24:506–13.
13. Ho MM, Ng AV, Lam S, Hung JY. Side population in human lung cancer cell lines and tumors is enriched with stem-like cancer cells. Cancer Res 2007;67:4827–33.
14. Wu C, Alman BA. Side population cells in human cancers. Cancer Lett 2008;268:1–9.
15. Sauvageau M, Sauvageau G. Polycomb group genes: keeping stem cell activity in balance. PLoS Biol 2008;6:e113.
16. Lee TI, Jenner RG, Boyer LA, Guenther M, Levine SS, Kumar RM, et al. Control of developmental regulators by Polycomb in human embryonic stem cells. Cell 2006;125:301–13.
17. Boyer LA, Lee TI, Cole MF, Johnstone SE, Levine SS, Zucker JP, et al. Core transcriptional regulatory circuitry in human embryonic stem cells. Cell 2005;122:947–56.
18. Suva ML, Riggi N, Janiszewska M, Radovanovic I, Provero P, Stehle JC, et al. EZH2 is essential for glioblastoma cancer stem cell maintenance. Cancer Res 2009;69:9211–18.
19. Simon JA, Lange CA. Roles of the EZH2 histone methyltransferase in cancer epigenetics. Mutat Res 2008;647:21–29.
20. Cao R, Zhang Y.The functions of E(Z)/EZH2-mediated methylation of lysine 27 in histone H3. Curr Opin Genet Dev 2004;14:155–64.
21. Matsukawa Y, Semba S, Kato H, Ito A, Yanagihara K, Yokozaki H. Expression of the enhancer of zeste homolog 2 is correlated with poor prognosis in human gastric cancer. Cancer Sci 2006;97:484–91.
22. Bryant RJ, Cross NA, Eaton CL, Hamdy FC, Cunliffe VT. EZH2 promotes proliferation and invasiveness of prostate cancer cells. Prostate 2007;67:547–56.
23. Collett K, Eide GE, Arnes J, Stefansson IM, Eide J, Braaten A, et al. Expression of enhancer of zeste homologue 2 is significantly associated with increased tumor cell proliferation and is a marker of aggressive breast cancer. Clin Cancer Res 2006;12:1168–74.
24. Karanikolas BD, Figueiredo ML, Wu L. Polycomb group protein enhancer of zeste 2 is an oncogene that promotes the neoplastic transformation of a benign prostatic epithelial cell line. Mol Cancer Res 2009;7:1456–65.
25. Nikoloski G, Langemeijer SM, Kuiper RP, Knops R, Massop M, Tonnissen ER, et al. Somatic mutations of the histone methyltransferase gene EZH2 in myelodysplastic syndromes. Nat Genet 2010;42:665–7.
26. Rao ZY, Cai MY, Yang GF, He LR, Mai SJ, Hua WF, et al. EZH2 supports ovarian carcinoma cell invasion and/or metastasis via regulation of TGF–{beta}1 and is a predictor of outcome in ovarian carcinoma patients. Carcinogenesis 2010;31:1576–83.
27. Hu S, Yu L, Li Z, Shen Y, Wang J, Cai J, et al. Overexpression of EZH2 contributes to acquired cisplatin resistance in ovarian cancer cells *in vitro* and *in vivo*. Cancer Biol Ther 2010 Oct 7;10: [Epub ahead of print].

28. Benard J, Da Silva J, De Blois MC, Boyer P, Duvillard P, Chiric E, et al. Characterization of a human ovarian adenocarcinoma line, IGROV1, in tissue culture and in nude mice. Cancer Res 1985: 45:4970–79.
29. Langdon SP, Lawrie SS, Hay FG, Hawkes MM, McDonald A, Hayward IP, et al. Characterization and properties of nine human ovarian adenocarcinoma cell lines. Cancer Res 1988:48:6166–72.
30. Workman P, Balmain A, Hickman JA, McNally NJ, Rohas AM, Mitchison NA, et al. UKCCCR guidelines for the welfare of animals in experimental neoplasia. Lab Anim 1988;22:195–201.
31. Irizarry RA, Hobbs B, Collin F, Beazer-Barclay YD, Antonellis KJ, Scherf U, et al. Exploration, normalization, and summaries of high density oligonucleotide array probe level data. Biostatistics 2003; 4:249–64.
32. Subramanian A, Tamayo P, Mootha VK, Mukherjee S, Ebert BL, Gillette MA, et al. Gene set enrichment analysis: a knowledge-based approach for interpreting genome-wide expression profiles. Proc Natl Acad Sci U S A 2005;102:15545–50.
33. Efron B, Tibshirani R. On testing the significance of sets of genes. Stanford tech report rep . 2006. Available from:http://www-stat.stanford.edu/~tibs/ftp/GSA.pdf.
34. Neumuller RA, Knoblich JA. Dividing cellular asymmetry: asymmetric cell division and its implications for stem cells and cancer. Genes Dev 2009;23:2675–99.
35. Dean M, Fojo T, Bates S. Tumour stem cells and drug resistance. Nat Rev Cancer 2005;5:275–284.
36. Ikuta K, Takemura K, Sasaki K, Kihara M, Nishimura M, Ueda N, et al. Expression of multidrug resistance proteins and accumulation of cisplatin in human non-small cell lung cancer cells. Biol Pharm Bull 2005;28:707–12.
37. Nomura M, Matsunami T, Kobayashi K, Uchibayashi T, Koshida K, Tanaka, M, et al. Involvement of ABC transporters in chemosensitivity of human renal cell carcinoma, and regulation of MRP2 expression by conjugated bilirubin. Anticancer Res 2005;25:2729–35.
38. Weaver DA, Crawford EL, Warner KA, Elkhairi F, Khuder SA, Willey JC. ABCC5, ERCC2, XPA and XRCC1 transcript abundance levels correlate with cisplatin chemoresistance in non-small cell lung cancer cell lines. Mol Cancer, 2005;4:18–22.
39. Christgen M, Geffers R, Ballmaier M, Christgen H, Poczkaj J, Krech T, et al. Down-regulation of the fetal stem cell factor SOX17 by H33342: a mechanism responsible for differential gene expression in breast cancer side population cells. J Biol Chem 2010;285:6412–18.
40. Margueron R, Justin N, Ohno K, Sharpe ML, Son J, Drury WJ, et al. Role of the polycomb protein EED in the propagation of repressive histone marks. Nature 2009;461:762–67.
41. Shen X, Liu Y, Hsu YJ, Fujiwara Y, Kim J, Mao X, et al. EZH1 mediates methylation on histone H3 lysine 27 and complements EZH2 in maintaining stem cell identity and executing pluripotency. Mol Cell 2008;32:491–502.
42. Kondo Y, Shen L, Cheng AS, Ahmed S, Boumber Y, Charo C, et al. Gene silencing in cancer by histone H3 lysine 27 trimethylation independent of promoter DNA methylation. Nat Genet, 2008; 40:741–50.
43. Abbosh PH, Montgomery JS, Starkey JA, Novotny M, Zuhowski EG, Egorin MJ, et al. Dominant-negative histone H3 lysine 27 mutant derepresses silenced tumor suppressor genes and reverses the drug-resistant phenotype in cancer cells. Cancer Res 2006;66:5582–91.
44. Wei Y, Xia W, Zhang Z, Liu J, Wang H, Adsay NV, et al. Loss of trimethylation at lysine 27 of histone H3 is a predictor of poor outcome in breast, ovarian, and pancreatic cancers. Mol Carcinog 2008;47: 701–6.
45. Chang Y, Zhang X, Horton JR, Upadhyay AK, Spannhoff A, Liu J, et al. Structural basis for G9a-like protein lysine methyltransferase inhibition by BIX-01294. Nat Struct Mol Biol 2009;16:312–17.
46. Tan J, Yang X, Zhuang L, Jiang X, Chen W, Lee PL, et al. Pharmacologic disruption of Polycomb-repressive complex 2-mediated gene repression selectively induces apoptosis in cancer cells. Genes Dev 2007;21:1050–63.